PROCEEDINGS, Twenty-Fifth Workshop on Geothermal Reservoir Engineering
Stanford University, Stanford, California, January 24-26, 2000
SGP-TR-165

AN EXAMINATION OF SIGNAL PROCESSING METHODS FOR MONITORING UNDISTURBED GEOTHERMAL RESOURCES

J D Leaver[1] A Watson[2] G Timpany[3] J Ding[1]

[1] UNITEC Institute of Technology, Private Bag 92025, Auckland, N.Z.
[2] Geothermal Institute, University of Auckland, Private Bag 92019, Auckland, N.Z.
[3] National Institute of Water and Atmospheric Research, Private Bag 99940, Auckland, N.Z.
jleaver@unitec.ac.nz

ABSTRACT

Water level data from a shallow monitor well in the Rotorua geothermal field in New Zealand is used to compare signal processing techniques, namely discrete Fourier transform and wavelet analyses. Characteristic pressure fluctuations are identified over a wide range of frequencies indicative of influences that include tides due to celestial bodies. The techniques used for data analysis provide complimentary information on characteristic fluctuations.

INTRODUCTION

Subsurface fluid reservoirs demonstrate fluctuations in reservoir temperature and pressure with time. In general these will be either cyclic due to tidal effects, seasonal changes or other regular disturbances, or pseudo-random due to the nature of the flow through the reservoir.

The pseudo-random fluctuations may reveal information about the nature of the permeability, fluid phases and other “micro” reservoir processes which could assist in characterising the flow through the reservoir and hence the existing state of natural systems. There is concern, at least in New Zealand, that there is no means of establishing whether the use of a geothermal resource for production is damaging natural features except to monitor it for several years and watch for significant changes. This investigation is to discover whether earlier detection of effects is possible before they become apparent to the casual observer. The first step in examining this is to check the sensitivity of available instrumentation and develop the analytical techniques. This paper reports progress on these using geothermal aquifer pressure measurements at Rotorua.

The Rotorua geothermal field is located near the centre of the North Island of New Zealand within the Taupo Volcanic zone. This zone extends from the central North Island mountains of Ngaruhoe, Ruapehu and Tongariro to the north east coast in an equilateral triangle with a chord length of about 200 km.

Data collected in Rotorua is part of a monitoring programme started in the early 1980’s designed to ensure that exploitation of the local geothermal resource by shallow geothermal wells would not have a significant negative impact on the thermal features of the Whakarewarewa geothermal field in Rotorua. This field features the Pohutu Geyser one of New Zealand’s best known tourist attractions. The scheme adopted is to measure the water level in a monitor well located about a kilometre from Pohutu Geyser. The water level indicates the pressure in the aquifer supplying the geyser. If the water level decreases to a predetermined level defined as critical, the production wells in the area must be closed.

DATA COLLECTION

Data was collected from monitor well RR777-M6 located at 1 Goodwin Ave., Rotorua. For the first 18 days of data a pressure transducer with an accuracy of +/-10 mm was used. After 18 days the transducer was replaced with a float and counterweight system connected to a rotary shaft encoder with an accuracy of +/-1 mm in water level. Rainfall was also measured, and barometric pressure was recorded using a KDG ACT 308 sensor with a range of 900 to 1050 mbars. All measurements were logged at hourly intervals. The sensors and logger were made by National Institute for Water and Atmospheric Research (NIWA). Data from well R777 covering a 2 year period from 2pm 30 June 1996 is shown in Figure 1.

Determination of the absolute pressure level in the aquifer from water level measurements requires a knowledge of the temperature distribution in the well. This was assumed to be constant for this study.

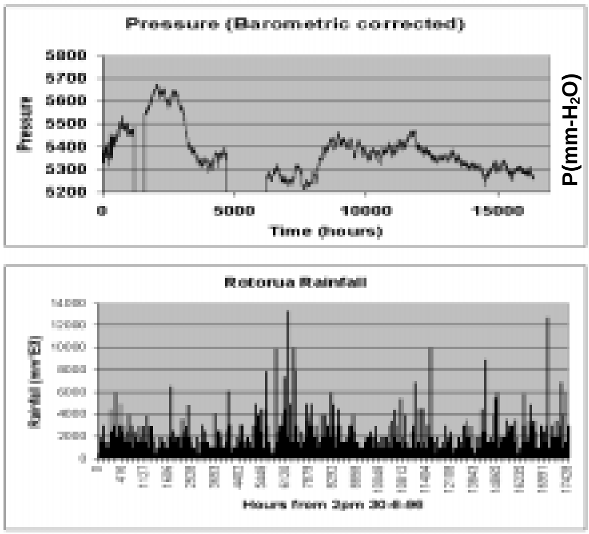

Fig. 1. Water level and rainfall records for well RR777.

The discharge period of the Pohutu Geyser is variable but of the order of 1 hour. As this is the same as the logging interval the data analysis unfortunately cannot be used to detect the effect of Pohutu on the monitor well water level.

METHODS OF ANALYSIS

Power Spectral Density

Measurements of geothermal surface activity or downhole pressures to detect changes due to production must be carried out over a long period of time. Hence they must be digitised signals. Digital signal analysis methods have been under development for the last 30 years. Since the data stream is random or pseudo-random, there is no single frequency component representation of the signal. The frequency components present at any time follow a Gaussian (or other) distribution and represent physical processes. The power spectral density of the signal is the Fourier transform of the autocorrelation function. In practice the signal is Fourier transformed directly rather than via the autocorrelation function using the fast Fourier transform algorithm.

The Fourier transform is:

$$F(\omega) = \frac{1}{2\pi} \int_{-\infty}^{\infty} f(t) e^{-i\omega t} dt \qquad (1)$$

Wavelet Transform

Wavelet analysis provides a way of decomposing a signal into its constituent parts using a compact waveform. The signal is broken up into scaled and translated versions of the wavelet. Analysis can be performed with either a continuous (CWT) or discrete wavelet transform (DWT). The CWT is continuous in that the analysing wavelet is shifted smoothly over the signal domain. The CWT can also operate at every scale from that of the original signal to a specified maximum.

The DWT operates on scales and translation positions which are dyadic (i.e. power of two). Computational effort is substantially reduced with DWT. Processing is further enhanced if a fast wavelet transform algorithm is used (Mallat, 1989). One-dimensional analysis involves signal decomposition by a family of orthogonal analysing wavelets. Orthogonal wavelets are derived from scaling functions (Appendix 1).

The wavelet transform coefficients depend on scale and amplitude. The magnitude of these coefficients represents a form of correlation between the signal and wavelet and are calculated by:

$$C(d, e) = d^{-0.5} \int_{-\infty}^{\infty} \Psi\left(\frac{x-e}{d}\right) f(x) dx \qquad (2)$$

where Ψ is the wavelet function and d, *e*, are dyadic scale and translation factors respectively.

DISCUSSION

Fourier Analysis

Windowed fast Fourier analysis was performed on data available during the first 10,335 hours (14 months). This was divided into 512 point blocks (21 days) in order to locate cyclic events that occur only over parts of the signal (Figure A1).

For a data record length of 512 hours, a period of 12 hours corresponds to a frequency of 43 with a 24 hour period having a frequency of about 21. Both of these periods are evident in every window except

Window (Hours)	Dominant Periods (Hours)
1-512	64, 102
514-1025	12, 24, 84
2114-2625	12, 24, 128
3653-4164	12, 24, 57, 128
4166-4678	12, 24, 57, 170
6233-6744	12, 24
6746-7257	12, 24, 57,
8285-8786	12, 24, 73
8798-9309	12
9311-9822	12, 24, 128
9824-10335	12, 24
6365-16364	8, 12, 24

Table 1. Dominant periods from windowed Fourier analysis

one. Two other periods are evident in 3 of the 11 windows. These occur at 57 hours and 128 hours.

Fourier analysis of a large window of data from 6365 hours to 16364 hours is shown in Fig. A2. The dominant periods are 8, 12 and 24 hours. The significance of the characteristic periods apart from the relation to celestial body cycles at 12 and 24 hours is not yet apparent.

Wavelet Analysis

Wavelet analysis in this study uses one of the family of orthogonal and compactly supported wavelets. These include the wavelet types of Daubechies (dbN), symlets (symN), and coiflets (coifN).

General properties of this family are that they are based on a scaling function that has a given number of vanishing moments and the analysis is orthogonal. Both the scaling function and the wavelet function are compactly supported. These properties are conducive to both continuous and discrete wavelet transform analysis due to the numerical efficiency generated as a result of orthogonality.

The wavelet used to analyse Rotorua data is the order 5 "coif5" wavelet (Figure 2) developed by Coifman et al. (1992). This wavelet was chosen because of its

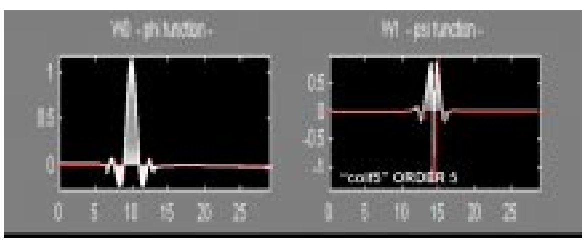

Fig. 2. Profile of 'coif5' wavelet

ability to model sharp points in the data and its analytical efficiency. The scaling and wavelet functions have a support width of 6N-1, and length of 6N. They also have 2N-1 and 2N vanishing moments respectively.

A 12 level wavelet decomposition was performed (Figures A3 and A4) on the water level data after correction for barometric effects. The wavelet decomposition breaks down the signal into 12 Details and an Approximation. The sum of these components reconstructs the original signal. The finest details of the signal are shown in Details 1 with coarsest trend shown in Approximation A12. The resulting wavelet Details were subjected to Fourier analysis to identify characteristic frequencies (Figures A5 and A6). The dominant characteristic wavelet periods are shown in Table 2.

Detail No.	**Dominant Periods (Hours)**
1	-
2	6, 8
3	6, 8, 12,
4	24
5	43
6	84

Table 2. Dominant periods from wavelet Details.

A detailed interpretation is outside the scope of this paper however in comparing Tables 1 and 2 and Figures A2 and A6 Fourier analysis of the wavelet Details identifies a characteristic frequency at 6 hours that is not apparent in the analysis using Fourier alone. This is probably because the wavelet based decomposition of the signal extracts fine "details" prior to the application of Fourier analysis. This prevents the masking of these components during Fourier analysis on the raw data set.

A theoretical calculation of the tides at Rotorua due to the solar system and moon is shown as Fig 3.

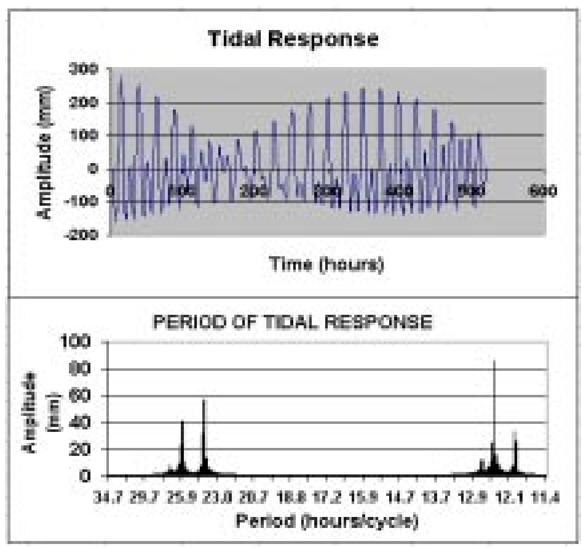

Fig. 3. Calculated tidal response at Rotorua

From Figure A1 the dominant periods are 12 and 24 hours, which compare very favourably with Fig. 2.

CONCLUSIONS

The analysis techniques reviewed reveal that the combination of conventional Fourier analysis with wavelet analysis can provide greater clarity in the detection of characteristic pressure fluctuations than using Fourier analysis alone. Much more detailed analysis is required to examine the significance of the fluctuations noticed.

ACKNOWLEDGEMENTS

The authors gratefully acknowledge Derek Goring, NIWA, for the provision of tidal data. Funding assistance was provided by UNITEC Institute of Technology and the University of Auckland.

REFERENCES

Coifman, R.R., Wickerhauser, M.V. (1992). "Entropy-based Algorithms for Best Basis Selection". *IEEE Trans. On Inf. Theory*, Vol. 38, 2, pp. 713 – 718.

Davis J.C. (1973) "Statistics and Data Analysis in Geology", John Wiley & Sons, Inc.

Hubbard B.B. (1998). "The World According to Wavelets", A K Peters, Wellesley-MA.

Leaver, J.D., Watson, A., Ding, J.J. (1999), "Application of Fourier and Wavelet Analyses to Pressure Data from the Te Aroha Hydrothermal System", *Proc. 21st N.Z. Geothermal Workshop,* pp. 211-216.

Mallat S. (1989). "A Theory for Multiresolution Signal Decomposition: The Wavelet Representation", *IEEE Pattern Anal. and Machine Intell.*, Vol. 11, No. 7, pp 674-693.

Newlands, D.E. (1993). "An Introduction To Random Vibrations, Spectral & Wavelet Analysis". Addison Wesley Longman Ltd, Essex.

Spiegel M.R. (1974), "Fourier Analysis with Applications to Boundary Value Problems", McGraw-Hill.

The MathWorks. (1984-1998). MATLAB The Language of Technical Computing.

Torrence, C., Compo G.P. (1998) "A Practical Guide to Wavelet Analysis", *Bull. Am. Met. Soc.:* Vol. 79, No. 1, pp. 61-78.

APPENDIX 1

The wavelet transform is profound in both its complexity of development and simplicity of application. For those not familiar with the development of wavelets a brief overview of wavelet formulation based on mathematical development of Newlands (1993), follows:

- Choose "seed" function $\phi_0(x)$.
- Choose number of coefficients to be used in the dilation equation.
- Calculate dilation coefficients, c_k, that satisfy 3 conditions:

(i) Accuracy

$$\sum_{k=0}^{N-1} (-1)^k k^m c_k = 0 \qquad \text{(A1)}$$

(ii) Conservation of (unit) area of scaling function.

$$\sum_{k=0}^{N-1} c_k = 2 \qquad \text{(A2)}$$

(iii) Orthogonality of the wavelet system.

$$\sum_{k=0}^{N-1} {c_k}^2 = 2 \qquad \text{(A3)}$$

$$\sum_{k=0}^{N-1} c_k c_{k+2m} = 0 \qquad m \neq 0 \qquad \text{(A4)}$$

- Iterate for scaling function, $\phi(x)$, using the dilation equation

$$\phi(x) = \sum_{k=0}^{N-1} c_k \phi(2x-k) \qquad \text{(A5)}$$

- Iterate for the wavelet function, $W(x)$, using the iterated scaling function $\phi(x)$.

$$W(x) = \sum_{k=0}^{N-1} (-1)^k c_k \phi(2x+k-N+1) \qquad \text{(A6)}$$

- Use the discrete wavelet transform

$$f(x) = \sum_{k=-\infty}^{\infty} c_{\phi,k} \phi(x-k) + \sum_{j=0}^{\infty} \sum_{k=-\infty}^{\infty} c_{j.k} W(2^j x - k) \qquad \text{(A7)}$$

Or assuming wrapping around the interval $0 \leq x < 1$ the above equation can be rewritten as:

$$f(x) = a_0 \phi(x) + \sum_{j=0}^{\infty} \sum_{k=-\infty}^{\infty} a_{2^j+k} W(2^j x - k) \qquad \text{(A8)}$$

Where a's are the amplitudes of the contributing wavelets which can be determined by orthogonality conditions:

$$a_0 = \int_0^1 f(x)\phi(x)dx \qquad \text{(A9)}$$

$$a_{2^j+k} = 2^j \int_0^1 f(x)\Psi(2^j x - k)dx \qquad \text{(A10)}$$

The amplitudes can be calculated using Mallat's algorithm (Mallat 1989).

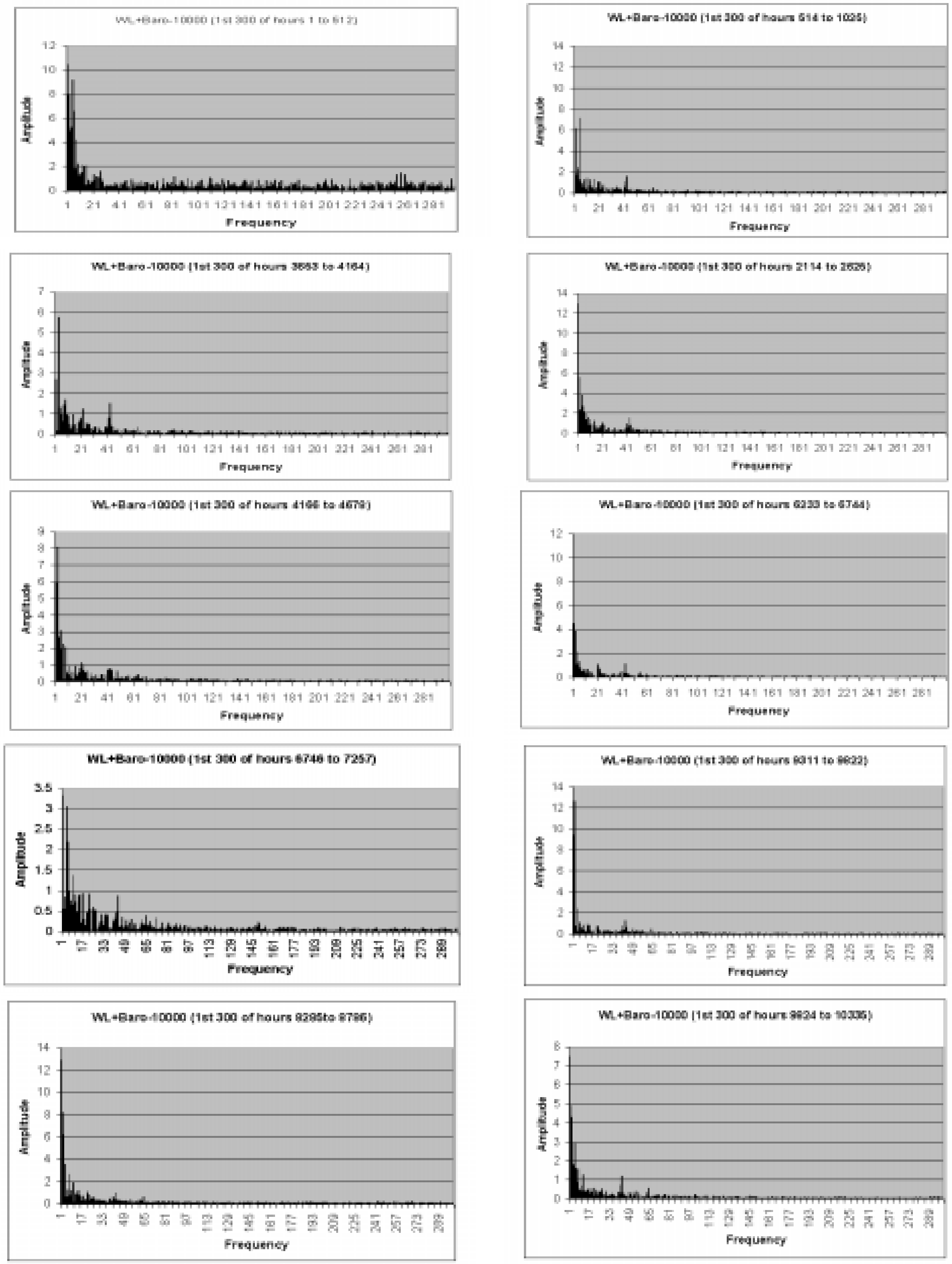

Fig. A1. Windowed Fourier Analysis of water levels after barometric correction

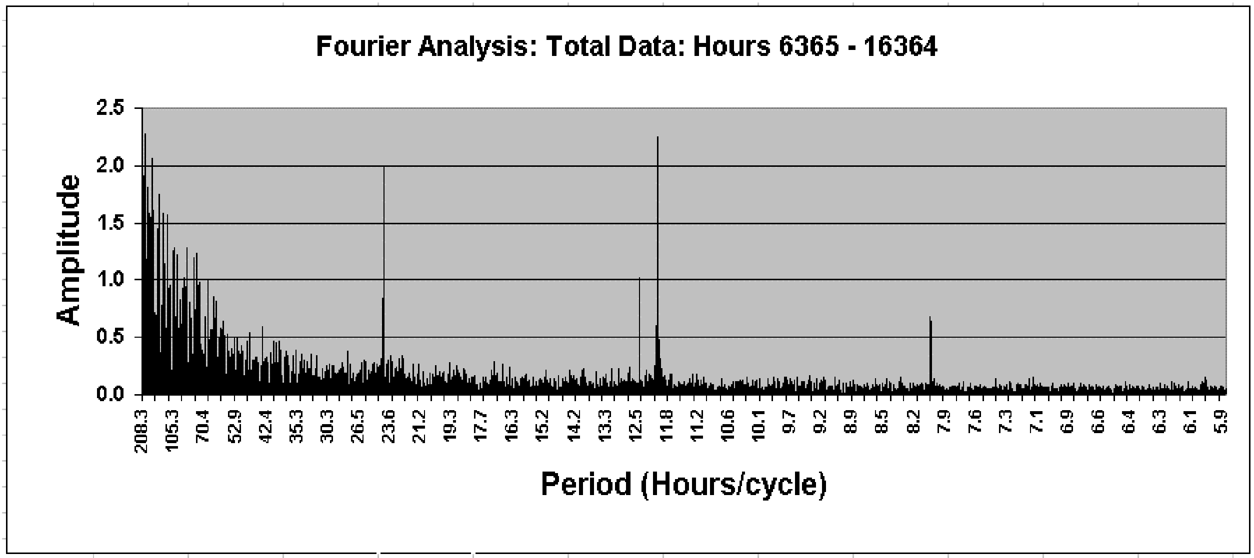

Fig. A2. Large window Fourier Analysis of data after barometric correction.

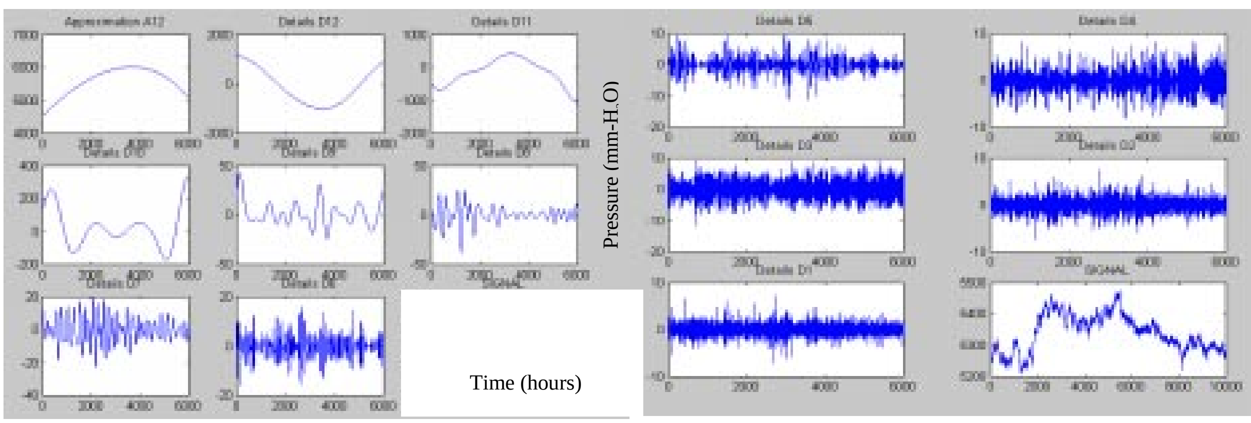

Fig. A3. “Coif 5” 12 level wavelet decomposition of water level after barometric correction: Hours 6364 - 16363: (Zoom Hours 8364-14363)

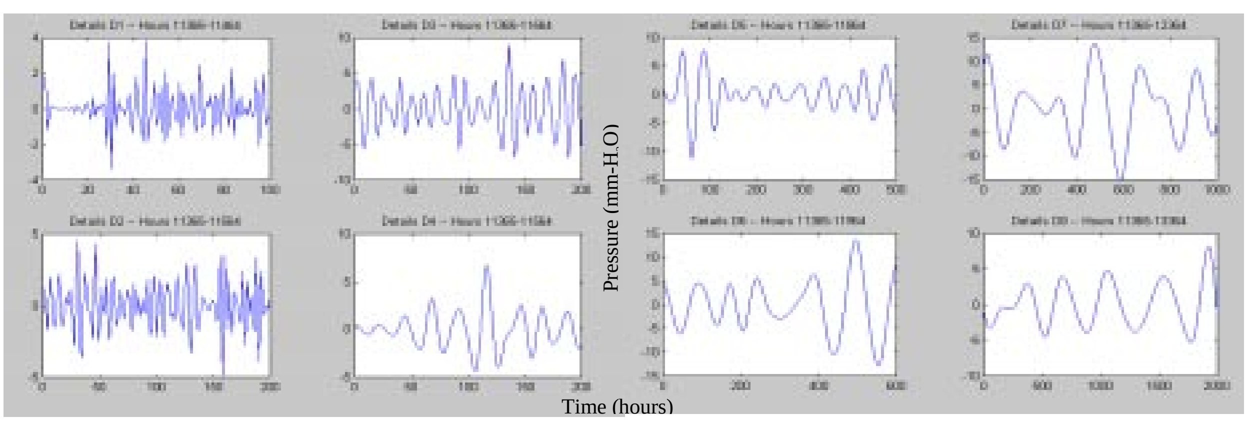

Fig. A4. Zoomed sections of “Coif 5” 12 level wavelet decomposition of water level after barometric correction: Hours 6364 - 16363: (Zoom hours shown)

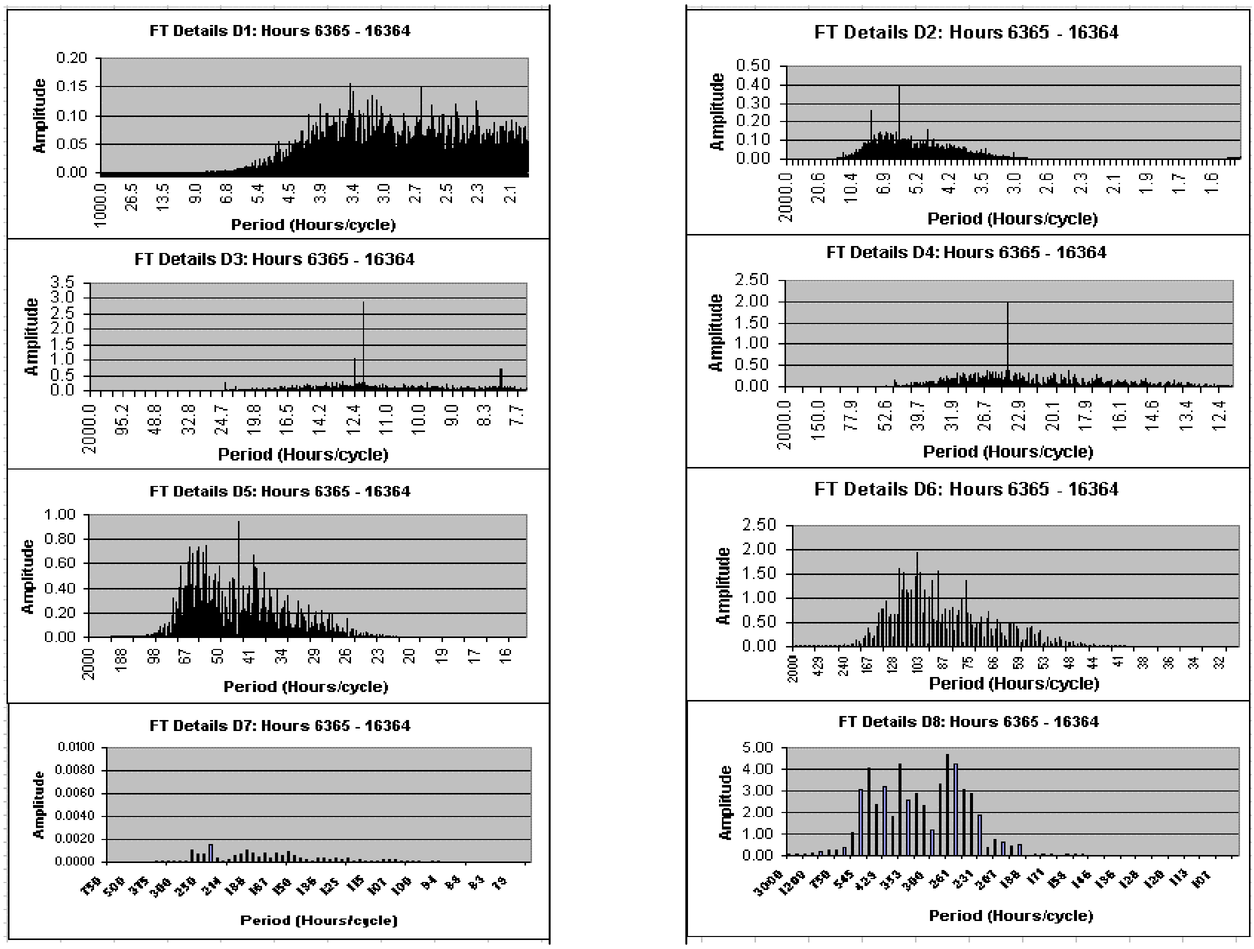

Fig. A5. Fourier analysis of details D1-D8 hours 8364-14363 except for D1 for which analysis is hours 9864 - 12863.

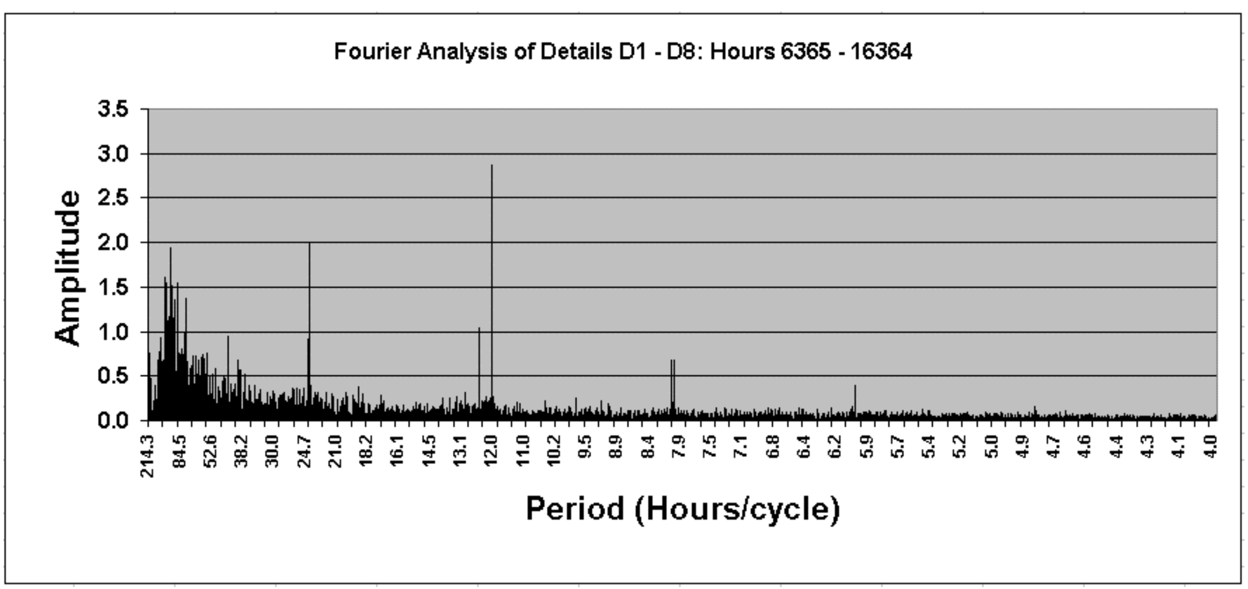

Fig. A6. Combined results of Fourier analysis of details D1-D8 hours 8364-14363 except for D1 for which analysis is hours 9864 - 12863.